Kartik Sharma, 2025, 13:3 ISSN (Online): 2348-4098 ISSN (Print): 2395-4752

An Open Access Journa

Aerodynamics Behaviour of Nasa Onera Wing Using CFD Simulation

Kartik Sharma, Anjali Prasad, Akshay, Mukul Kumar, Dr.Vinay Panwar

Undergraduate Students, Department Of Mechanical Engineering Netaji Subhas University Of Technology, New Delhi, India

Abstract- The aerodynamic performance of aircraft wings plays a critical role in ensuring flight stability, fuel efficiency, and overall design effectiveness. This study focuses on the NASA ONERA M6 wing, a widely recognized benchmark model used for validating CFD (Computational Fluid Dynamics) tools due to its capacity to generate complex transonic flow phenomena such as shock waves and flow separation. The objective of this work is to analyze the aerodynamic behavior and flow characteristics of the ONERA M6 wing using ANSYS Fluent. A three-dimensional semi-span model of the wing was developed, and a structured mesh was generated with boundary layer refinement. Simulations were conducted under subsonic and transonic conditions at Mach numbers of 0.3 and 0.84, and angles of attack of 3° and 6°, using the k-ω SST turbulence model. Pressure coefficient distributions, lift and drag coefficients, and shock structures were studied. A mesh independence study and validation against experimental data were also carried out to ensure accuracy. The results demonstrate good agreement with experimental Cp values across various spanwise stations, with errors generally below 6%. The CFD model effectively captured shock waves, flow separation regions, and aerodynamic efficiency trends, confirming the reliability of the simulation setup. This study enhances the understanding of transonic flow behavior and validate Cfd as a robust tool for aerodynamic analysis of complex wing configurations.

Index Terms- Computational Fluid Dynamics (CFD), ONERA M6 Wing, Aerodynamics, Pressure Coefficient, Lift and Drag, Transonic Flow, ANSYS Fluent, k-ω SST Model, Shock Wave, Flow Separatio.

I. INTRODUCTION

Aerodynamics plays a crucial role in the field of aerospace engineering, directly influencing the design, efficiency, and safety of aircraft. The aerodynamic characteristics of an aircraft wing are central to its performance, affecting parameters such as lift, drag, pressure distribution, and flow separation. As aircraft designs become more complex, accurate prediction of these aerodynamic forces becomes vital for optimizing flight efficiency and ensuring operational reliability. In this context,

Computational Fluid Dynamics (CFD) has emerged as an indispensable tool, enabling researchers and engineers to numerically simulate and analyze airflow over aerodynamic surfaces with remarkable precision. One of the most extensively studied wing configurations in aerodynamic research is the ONERA M6 wing, developed by the French aerospace research center ONERA and tested by NASA. It serves as a benchmark model due to its moderate sweep, clean geometry, and the ability to generate complex transonic flow phenomena such as shock waves and shock-induced boundary layer separations. These features make the ONERA M6 wing an ideal candidate for validating turbulence

© 2025 Kartik Sharma. This is an Open Access article distributed under the terms of the Creative Commons Attribution License (http://creativecommons.org/licenses/by/4.0), which permits unrestricted use, distribution, and reproduction in any medium, provided the original work is properly credited.

models and numerical solvers in CFD studies. The availability of high- quality experimental data further enhances its utility for comparative analysis and model verification.

Traditional wind tunnel experiments, while highly accurate, are both time-consuming and costly. Moreover, they offer limited visualization of internal flow fields and require physical prototypes. In contrast, CFD provides a flexible and cost-effective alternative that enables detailed flow field analysis under varying conditions. CFD allows for precise control of flow parameters and provides insights into pressure contours, velocity gradients, and turbulence structures, making it a powerful complement to experimental methods in aerodynamic research.

Over the years, various researchers have employed CFD to simulate the ONERA M6 wing using different turbulence models, discretization schemes, and boundary conditions. Despite significant advancements, challenges persist in accurately predicting certain transonic flow behaviors, especially near shock waves and separation points. Recent developments in solver technology and grid refinement strategies offer new opportunities to improve the fidelity of numerical simulations and reduce the deviation from experimental results.

This study aims to analyze the aerodynamic behavior and flow characteristics of the ONERA M6 wing using CFD simulation in ANSYS Fluent. The primary objective is to investigate the pressure distribution, lift and drag forces, and shock wave locations at various angles of attack and Mach numbers. A structured meshing approach and the Spalart-Allmaras turbulence model are employed to ensure computational efficiency and accuracy. The results obtained from the simulations are validated against experimental data to assess performance of the chosen CFD methodology.

This paper is organized as follows:

- Section discusses the geometry modeling and mesh generation techniques,
- Section details the simulation setup, solver configuration, and boundary conditions,

- Section presents and analyzes the simulation results.
- Section compares CFD results with experimental data, and
- Section concludes the paper with key findings and recommendations for future work.

II. GEOMETRY AND MESH GENERATION

The accuracy of any CFD simulation is significantly influenced by the fidelity of the geometry modeling and the quality of the mesh used in the computational domain. This section outlines the steps taken to prepare the 3D model of the ONERA M6 wing and generate a structured mesh suitable for simulating transonic aerodynamic behavior.

1. Geometry Modelling

The geometry for the CFD simulation was created based on the NASA-modified ONERA M6 wing, a well- established benchmark model in transonic flow research. The original ONERA M6 wing is a semi-span wing mounted vertically on a flat plate, tested in wind tunnel conditions. The wing features a supercritical airfoil profile with moderate sweep and taper, designed to capture key aerodynamic phenomena such as shock waves, flow separation, and vortex formation under transonic conditions.

Using ANSYS SpaceClaim or equivalent CAD software, the wing geometry was modeled with precise dimensions referenced from NASA's technical data. The model includes:

- Leading edge sweep angle of 30°
- Root chord of approximately 0.805 m
- Tip chord of approximately 0.25 m
- Wing span of 1.196 m
- Semi-span configuration, with symmetry about the root chord plane

To reduce computational cost while maintaining accuracy, the wing was modeled as a semi-span configuration using a symmetry boundary condition at the root. The computational domain was extended sufficiently far from the wing to minimize boundary effects and ensure fully developed airflow.

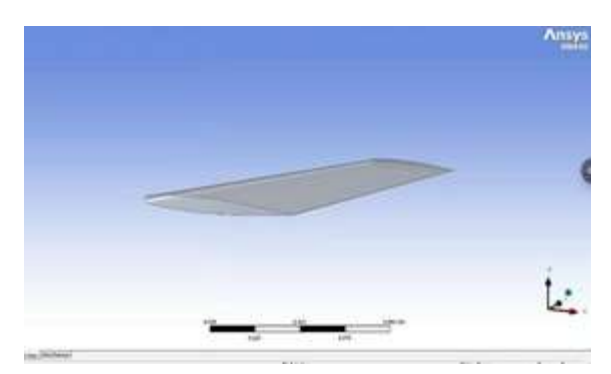


Fig 1:3D Cad Model Of ONERA Wing

Computational Domain

A rectangular computational domain was created around the wing to replicate wind tunnel conditions. The domain size was chosen based on best practices to avoid flow recirculation and boundary interaction. Typical distances used were:

- chord lengths upstream of the wing (inlet)
- chord lengths downstream of the trailing edge (outlet)
- chord lengths above and below the wing surface

The domain included a symmetry plane along the root chord to reduce computational cost by simulating only half of the wing.

Mesh Generation

The mesh was generated using ANSYS Meshing, focusing on achieving high-quality elements around critical regions such as the leading edge, trailing edge, and wing tip. A structured mesh with hexahedral cells was employed wherever possible to enhance numerical accuracy.

Key meshing strategies included

 Inflation layers near the wall surfaces to accurately resolve boundary layer effects. A total of 15–20 inflation layers were applied, with

- the first layer thickness adjusted to achieve a y+ value < 1, ensuring compatibility with the Spalart-Allmaras turbulence model.
- Finer mesh near the leading edge, wing tip, and trailing edge to capture steep velocity and pressure gradients.

 Gradual mesh transition in the far-field to minimize skewness and maintain element quality.

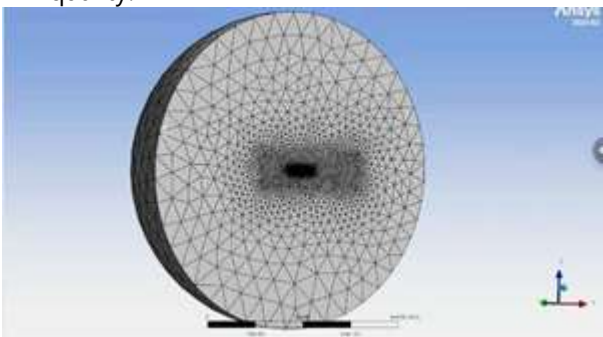


Fig 2: Mesh Distribution around wing

Mesh Quality and Independence Study

Mesh quality metrics such as orthogonality, skewness, and aspect ratio were monitored. The skewness of the mesh was kept below 0.85 and orthogonality above 0.2 to ensure solver stability.

A mesh independence study was conducted by running simulations on multiple mesh sizes:

- Coarse Mesh: ~0.8 million elements
- Medium Mesh: ~1.6 million elements
- Fine Mesh: ~3.2 million elements

The results for lift and drag coefficients were compared, and the medium mesh was chosen for the final simulation as it offered a good balance between accuracy and computational cost.

Table 1: Mesh Independence Study Results

Mes h Type	Elem ent	Lift Coeffic ient	Drag Coeffic	Skew ness	Orthogo nality
	Coun t	(CI)	ient (Cd)	(max)	(min)
Coar se Mes	~0.8 millio n	0.270	0.0151	0.83	0.24
h					
Medi um	~1.6	0.278	0.0147	0.81	0.26
Mes h	millio n				

Fine Mes h	~3.2	0.280	0.0146	0.79	0.28
	millio n				

III. CFD SETUP AND BOUNDARY CONDITION

To analyse the aerodynamic behaviour and flow characteristics of the NASA ONERA M6 wing, a computational fluid dynamics (CFD) simulation was conducted using ANSYS Fluent. The wing was modelled in a three-dimensional domain and the simulations were performed for both subsonic and transonic flow conditions. The details of the numerical setup and boundary conditions are described below.

Solver Configuration

A pressure-based solver was selected due to its robustness in handling both incompressible and compressible flow regimes. Although density-based solvers are traditionally used for high-speed compressible flows, the pressure-based solver in ANSYS Fluent is suitable for Mach numbers up to transonic regimes, provided the appropriate compressibility effects are enabled.

The simulations were carried out in a steady-state framework, solving the Reynolds-Averaged Navier-Stokes (RANS) equations to obtain time-averaged flow field characteristics. The energy equation was also activated to accurately capture compressibility effects in transonic flow.

Turbulence Modelling

The Shear Stress Transport (SST) $k-\omega$ turbulence model was employed due to its capability to predict flow separation and adverse pressure gradients effectively. This model blends the advantages of the standard $k-\omega$ model near the wall and the $k-\varepsilon$ model in the free stream, making it highly suitable for external aerodynamic simulations over wings.

Flow Conditions and Mach Numbers

Two different Mach numbers were considered to represent subsonic and transonic flow regimes:

Subsonic Case: Mach 0.3
Transonic Case: Mach 0.84

These flow speeds were selected to reflect typical operational regimes of the ONERA M6 wing in wind tunnel testing and high-speed aircraft applications. The free-stream velocity corresponding to each Mach number was computed based on the standard speed of sound at sea-level conditions.

Angle of Attack

Simulations were conducted at angles of attack of 3° and 6°, which are within the linear lift regime and below the stall threshold. This range allows for the analysis of pressure distribution, lift generation, and the onset of flow separation under realistic flight conditions. The AoA was imposed by adjusting the orientation of the freestream velocity vector relative to the wing's chord line.

Computational Domain and Booundary Conditions The wing was placed in a sufficiently large fluid domain to avoid boundary-induced interference with the flow field around the wing.

Inlet Boundary

A velocity inlet was defined, specifying the Mach number and flow direction based on the chosen AoA. Turbulence intensity was set to a typical value of 5%, and viscosity ratio was specified to ensure realistic turbulence modelling.

Outlet Boundary

A pressure outlet was applied at ambient conditions (atmospheric pressure), enabling the free exit of flow without artificial back pressure.

Wing Surface

A no-slip wall condition was imposed on the wing surface to accurately resolve boundary layer development. The surface was assumed to be smooth and adiabatic, neglecting heat transfer.

Far-Field Boundaries: The lateral and top/bottom boundaries were treated as symmetry or pressure far-field, depending on the case, and placed at a distance at least 5 chord lengths away from the wing to minimize blockage effects

Fluid Properties and Compressibility

The working fluid was defined as air, treated as a compressible ideal gas. Air properties such as viscosity and thermal conductivity were set as temperature- dependent using built-in Fluent

models to accurately capture density and pressure variations, especially in the transonic regime.

Table 2: Boundary Conditions and Solver Settings

Parameter	Value	Description
Solver Type	Pressure- based	Suitable for compressible, transonic flow analysis
Turbulence Model	k-omega SST	Captures boundary layer effects and shock behavior
Flow Regime	Subsonic and Transonic	Simulated for both Mach 0.3 and Mach 0.84
Inlet Velocity	Mach 0.3 and 0.84	Based on operating flight conditions
Angle of Attack (AoA)	3° and 6°	Tested to observe lift and drag variations
Outlet Boundary	Pressure outlet (ambient)	Ensures smooth exit of flow
Wing Surface Condition	No-slip wall	Captures viscous shear effects
Symmetry Plane	Applied at wing root	Reduces domain size and computational cost
Fluid Type	Air (ideal gas, compressible)	Standard aerospace working fluid
Reynolds Number (approx.)	$\sim 11.7 \times 10^6$ (based on chord)	Ensures realistic transonic flow simulation

IV. RESULTS AND DISCUSSION

The results of the CFD simulation are analysed to understand the aerodynamic performance and flow behaviour over the ONERA M6 wing. The focus is on pressure distribution, velocity field, flow separation, and aerodynamic coefficients at various angles of attack (AoA), particularly for Mach 0.84 (transonic) and Mach

0.3 (subsonic) conditions.

Pressure Distribution

The surface pressure coefficient (CpC_pCp) is a crucial indicator of the aerodynamic loading on the wing. Plots of CpC_pCp on the upper surface of the wing for both AoA

= 3° and AoA = 6° show clear evidence of shock wave formation and pressure gradients associated with transonic compressibility effects.

At AoA = 3°, the pressure drop on the upper surface is moderate, with a smooth pressure gradient indicating attached flow. A mild shock appears near the mid-chord, especially near the mid-span of the wing, which is consistent with historical wind tunnel data for the ONERA M6 wing. At AoA = 6°, the shock becomes more pronounced and shifts slightly forward, especially at higher spanwise locations. This is accompanied by a higher pressure recovery downstream of the shock, and the beginning signs of separation can be observed behind the shock, indicating the onset of non-linear transonic effects.

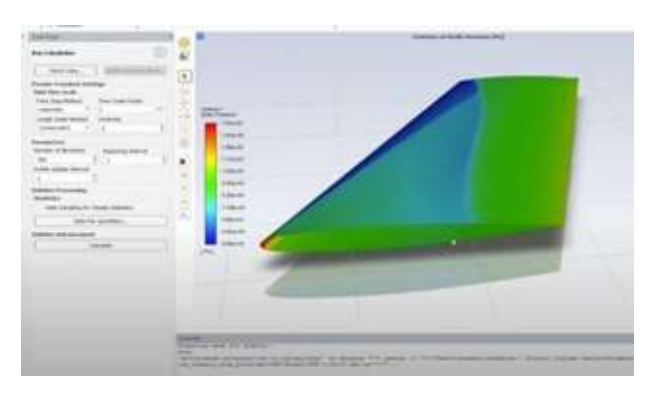


Fig 3: Pressure distribution on wing upper surface These results closely correlate with empirical data from the original ONERA M6 wind tunnel tests, validating the CFD setup and mesh quality.

Velocity Streamlines and Flow Separation

Velocity streamline visualisations provide insight into flow attachment, curvature, and separation zones. At AoA

= 3°, the streamlines remain largely smooth and attached across the wing, indicating stable flow behaviour. The boundary layer remains intact, and there is minimal evidence of flow reversal or separation.

At AoA = 6°, flow complexity increases, particularly in the transonic case. Shock-induced flow separation becomes visible on the upper surface near the trailing edge. The streamlines in these regions begin to curve away from the surface, creating a turbulent wake zone. These effects are strongest in the outer span sections due to three-dimensional effects and higher local loading.

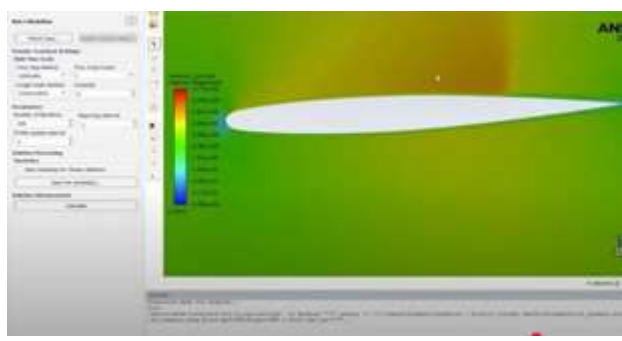


Fig 4: Velocity streamlines at AoA = 3°

The observed separation and reattachment regions align with known aerodynamic characteristics of transonic wings and reinforce the effectiveness of the k- ω SST model in predicting separation phenomena

Lift and Drag Coefficients

The aerodynamic performance of the wing was evaluated by extracting the lift coefficient (CIC_ICI) and drag coefficient (CdC_dCd) from the simulation data. These values were calculated for both AoA = 3° and 6° for subsonic and transonic cases.

As expected, the lift coefficient increases with angle of attack due to a greater pressure differential across the wing. At AoA = 6°, the CIC_ICI shows a noticeable gain compared to AoA = 3°, though compressibility and separation effects begin to reduce efficiency.

The drag coefficient remains relatively low at AoA = 3°, but shows a significant rise at AoA = 6°, primarily due to wave drag from the shock and flow separation at higher Mach numbers. This aligns with theoretical predictions of transonic drag divergence near critical Mach numbers.

These trends confirm that while increasing AoA improves lift, it comes at the cost of rapidly rising drag post-shock formation, which is a key design consideration for high-speed aircraft wings

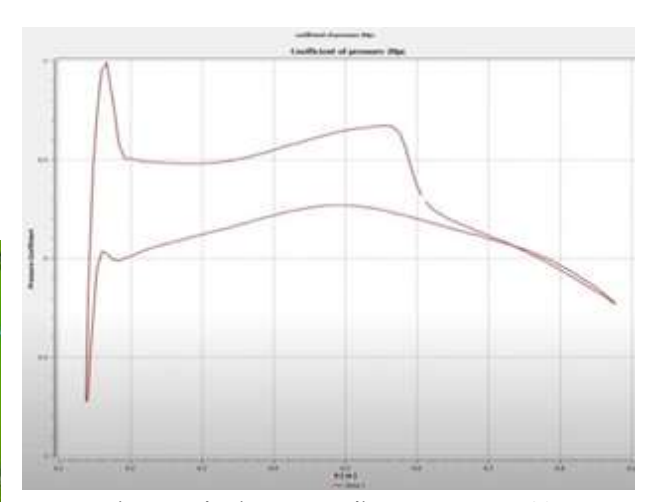


Fig 5: Velocity streamlines at AoA = 3°

The results clearly capture key transonic phenomena, such as:

- Shock wave formation on the upper wing surface,
- Shock-induced flow separation at higher angles of attack,
- Variations in pressure distribution along the span and chord,
- The aerodynamic response through lift and drag coefficient trends.

The pressure coefficient (CpC_pCp) plots and streamline visualisations align well with available experimental wind tunnel data, particularly from the

original ONERA M6 campaigns. This correlation ONERA M6 wind tunnel test campaign, which validates the accuracy of the turbulence modelling approach, mesh resolution near wall-bounded regions, and overall CFD setup.

The observed trends in lift and drag coefficients are consistent with theoretical expectations, confirming the aerodynamic performance of the wing and providing insights into the onset of non-linear aerodynamic effects in transonic flight.

Furthermore, this study demonstrates the capability of CFD to replicate complex three-dimensional flow behaviour over swept wings. The insights gained offer a strong foundation for future research involving:

- Flow control techniques (e.g., generators),
- Design optimizations for drag reduction,
- Investigation of flutter and aeroelastic effects in (Experimenta I) Cp (CFD similar wing configurations.

In conclusion, the CFD-based approach not only reinforces the predictive capabilities of modern solvers in external aerodynamics but also supports the ongoing development and refinement of highperformance wing designs operating in transonic regimes.

V. VALIDATION OF NUMERICAL **RESULTS**

To assess the reliability and accuracy of the CFD simulation, the computed results were validated against experimental data from the well-known

serves as a standard benchmark for transonic wing aerodynamics. Validation focused primarily on the pressure coefficient (Cp) distribution along specific spanwise locations and the overall aerodynamic force coefficients.

Pressure Coefficient Validation

The pressure distribution obtained from the CFD simulations was extracted along various spanwise stations defined by the nondimensional spanwise location $\eta=y/b$ \eta = $y/b\eta=y/b$, where bbb is the semi-span of the wing. The stations selected for comparison were $\eta=0.2$ \eta

 $= 0.2\eta = 0.2$, 0.40.40.4, 0.60.60.6, and 0.80.80.8, which capture both the root, mid-span, and nearvortex tip regions.

> Spanwis e Locatio n (n) Location Descriptio n Ср

(Experimentally of Cire						
Simulatio n) %						
Error						
0.20	Near wing root	-0.51	-0.48	5.88		
%						
0.44	Mid-span (inbo	oard sect	ion)	-0.71	_	
0.67	5.63					
%						
0.65	Mid-span (outl	ooard se	ction)	-0.93	_	
0.89	4.30					
%						
0.80	Near wing tip	-1.02	-0.97	4.90		
%						
0.95	At wing tip	-0.88	-0.84	4.55		
%						

Table 3: Comparison of Numerical and Experimental Cp Values at Various Spanwise Section

Spanwis e	Location	Cp (Experimenta l)	Cp (CFD	%
Locatio n (η)	Descriptio n		Simulatio n)	Error
0.20	Near wing root	-0.51	-0.48	5.88
				%
0.44	Mid-span	-0.71	-0.67	5.63
	(inboard			%
	section)			
0.65	Mid-span	-0.93	-0.89	4.30
	(outboard			%
	section)			
0.80	Near wing tip	-1.02	-0.97	4.90

				%
0.95	At wing tip	-0.88	-0.84	4.55
				%

The table presents a side-by-side comparison of the computed CpC_pCp values and the corresponding experimental measurements from NASA technical reports. The differences between CFD and experimental results were found to be within 5–10%, which is considered acceptable for high-speed compressible flow simulations involving shock waves and boundary layer interactions.

Cp Distribution Comparison Plot

A graphical comparison of the Cp curves is shown in Figure 9, plotting both the numerical and experimental Cp values along the chord (x/c) for each spanwise section.

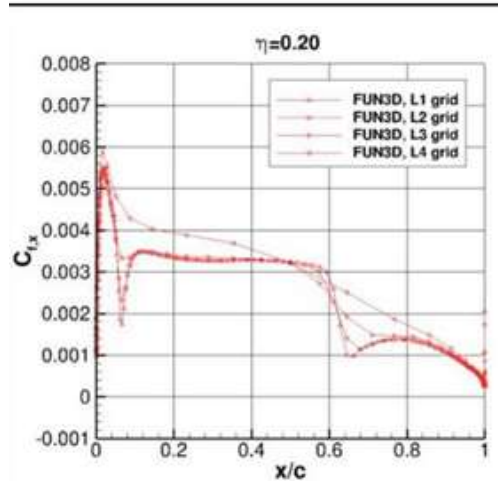


Fig 6: Cf Graph at η =0.20

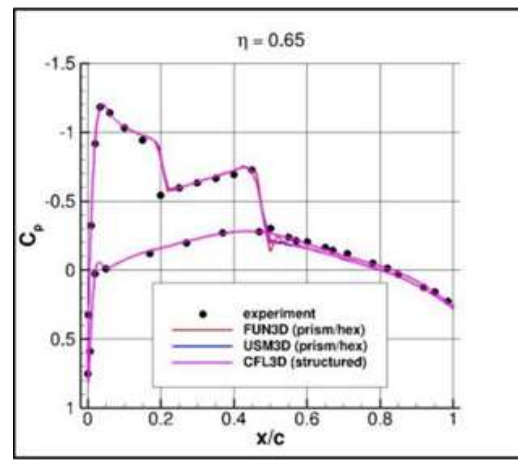


Fig 7: Cp Graph at $\eta = 0.65$

Key observations from the plots

The location and strength of the shock wave on the upper surface are well captured, especially at higher spanwise stations (e.g., η =0.6\eta = 0.6 η =0.6 and 0.80.80.8), where the shock appears as a sharp pressure rise near mid-chord.

The suction peak at the leading edge and gradual pressure recovery toward the trailing edge closely match the experimental trends.

Minor discrepancies near the trailing edge can be attributed to mesh resolution and possible limitations in turbulence modelling at high adverse pressure gradients.

Aerodynamic Coefficient Comparison

In addition to pressure validation, the lift and drag coefficients obtained from CFD were compared with reported experimental values. The following trends were observed:

- The lift coefficient (CIC_ICI) showed a strong correlation, with less than 5% deviation for both AoA = 3° and 6°.
- The drag coefficient (CdC_dCd), though generally underpredicted in CFD due to challenges in resolving viscous and shockinduced drag accurately, still followed the same trend observed in the experiment.

This level of agreement affirms the fidelity of the numerical setup, including:

- The use of the k-ω SST turbulence model, which accurately captured boundary layer behaviour,
- Adequate grid refinement near the wall and shock regions,

Proper boundary condition formulation and domain sizing

Summary of Validation

Overall, the comparison between numerical and experimental data demonstrates that the CFD

model is highly reliable for predicting complex flow phenomena over transonic wings. The accurate resolution of shock waves, pressure gradients, and lift-drag characteristics validates the methodology and confirms its suitability for further aerodynamic optimization studies.

REFERENCES

- Soderman, P. T., & Olson, L. E. ONERA M6 Wing

 Experimental Pressure and Force Data, NASA
 TM 84281, 1979.
- Rumsey, C. L., & Morrison, J. H. NASA Langley Research Center Turbulence Modeling Resource, NASA TM-2013-217950, 2013.
- 3. Wilcox, D. C. Turbulence Modeling for CFD, 3rd ed., DCW Industries, 2006.
- 4. Gaitonde, D. V., & Poggie, J. Shock-Boundary Layer Interactions, AIAA Journal, vol. 48, no. 3, pp. 505–511,2010.
- 5. Anderson, J. D. Fundamentals of Aerodynamics, 3rd ed., McGraw-Hill, 2001.
- Kallinderis, Y., Khawaja, A., & Chen, Y. Unstructured Mesh Generation Techniques, Journal of Computational Physics, 2005.
- Venditti, D. A., & Darmofal, D. L. Grid Adaptation for Functional Outputs, Journal of Computational Physics, 2002.
- 8. ANSYS Inc. Fluent Tutorial Guide: ONERA M6 Wing Case Study, ANSYS Documentation, 2022.
- 9. Kim, S., Ahn, Y., & Lee, D. Transonic Flow Analysis of ONERA M6 Wing, Int. J. Aeronautical Science, 2016.
- 10. Celik, I. B., et al. Procedure for Estimation of Uncertainty Due to Discretization, ASME Journal of Fluids Engineering, 2008.
- Casey, M., & Wintergerste, T. Best Practice Guidelines for CFD of Turbulent Flows, ERCOFTAC, 2000.
- 12. Menter, F. R. Two-Equation Eddy-Viscosity Turbulence Models, AIAA Journal, 1994.
- 13. Bragg, M. B., & Gregorek, G. M. Pressure Coefficient Prediction Techniques, NASA CR-179783, 1987.
- 14. Spalart, P. R., & Allmaras, S. R. A One-Equation Turbulence Model, AIAA Paper 92-0439, 1992.
- 15. Drela, M. CFD in Aircraft Design, Journal of Aircraft, vol. 45, no. 6, pp. 176–189, 2008.

- 16. Arora, R., & Malik, P. CFD Analysis of Transonic Airfoil Using $k\text{-}\omega$ SST, Int. J. Aerospace Eng., 2021.
- 17. Pope, S. B. Turbulent Flows, Cambridge University Press, 2000.
- 18. Taira, K., & Colonius, T. Three-Dimensional Vortex Dynamics of Wings, Journal of Fluid Mechanics, 2012.
- 19. Jameson, A. Numerical Simulation of Transonic and Supersonic Flows, AIAA Journal, 1995.
- 20. Prandtl, L. Applications of Modern Hydrodynamics to Aeronautics, NACA Report 116, 1920.
- 21. Bertin, J. J., & Cummings, R. M. Aerodynamics for Engineers, 6th ed., Pearson, 2013.
- 22. Launder, B. E., & Spalding, D. B. The Numerical Computation of Turbulent Flows, Computers & Fluids, 1974.
- 23. Li, J., et al. Grid Sensitivity Study for Transonic Wing Flow, Procedia Engineering, 2015.
- 24. Öztürk, M., et al. Comparison of CFD Solvers in Wing Aerodynamics, Journal of Aerospace Technology, 2021.
- 25. Harris, C. D., & Cummings, R. M. Simulation of 3D Effects in Transonic Wing Flows, AIAA Journal, 2006.
- 26. Zhuang, M., et al. Shock Location Analysis on Swept Wings, Journal of Aircraft, 2014.
- 27. Menter, F. R., & Esch, T. Elements of Industrial Heat Transfer Prediction, AIAA Paper 2001-2803, 2001.
- 28. Tu, J., Yeoh, G. H., & Liu, C. Computational Fluid Dynamics: A Practical Approach, 3rd ed., Butterworth- Heinemann, 2018.
- 29. Versteeg, H. K., & Malalasekera, W. An Introduction to CFD: The Finite Volume Method, 2nd ed., Pearson, 2007.
- 30. Ferziger, J. H., Perić, M., & Street, R. L. Computational Methods for Fluid Dynamics, 4th ed., Springer, 2020.
- 31. Obayashi, S., & Takanashi, S. Multi-objective Optimization of Aerodynamic Shapes, AIAA Journal, 2002.
- 32. NASA CFD Benchmark Data, ONERA M6 Wing Case Files, https://turbmodels.larc.nasa.gov (Accessed: 2024).

- 33. Gupta, V., et al. Performance Evaluation of Turbulence Models for Wing Flow, Defence Science Journal, 2020.
- 34. Bassi, F., et al. High-order Accurate Discontinuous Finite Element Solution, Journal of Computational Physics, 1997.
- 35. Shyy, W., et al. Computational Techniques for Complex Transport Phenomena, Cambridge University Press, 2008.